

ARTICLE

Bioinspired ultrathin photonic color convertors for highly efficient micro-light-emitting diodes

Jiexin Li¹ | Xinrui Ding¹ | Yuzhi Shi²  | Jiasheng Li¹ | Zihao Deng¹ |
Jiayong Qiu¹ | Jinhui Zhang³ | Wei Luo⁴ | Guanwei Liang⁵ | Long Zhao³ |
Yong Tang¹ | Ai Qun Liu⁴ | Zongtao Li^{1,3}

¹National & Local Joint Engineering Research Center of Semiconductor Display and Optical Communication Devices, South China University of Technology, Guangzhou, China

²Institute of Precision Optical Engineering, School of Physics Science and Engineering, Tongji University, Shanghai, China

³Guangdong Provincial Key Laboratory of Semiconductor Micro Display, Foshan Nationstar Optoelectronics Company Ltd., Foshan, China

⁴Department of Electrical and Electronic Engineering, Quantum Engineering and Science, The Hong Kong Polytechnic University, Hong Kong, China

⁵School of Fashion and Textiles, The Hong Kong Polytechnic University, Hong Kong, China

Correspondence

Jiasheng Li, Ai Qun Liu and Zongtao Li.

Email: jjasli@scut.edu.cn, aiqun.liu@polyu.edu.hk and meztli@scut.edu.cn

liu@polyu.edu.hk and meztli@scut.edu.cn

Funding information

National Key R & D Program of China, Grant/Award Number: 2021YFB3600205; National Natural Science Foundation of China, Grant/Award Number: 52105443; Guangdong Provincial Key R&D Program, Grant/Award Number: 2022B0101090002; National Science Foundation of Guangdong Province, Grant/Award Number: 2022A1515011059; National Key Research and Development Program of China, Grant/Award Number: 2023YFF0613600; Shanghai Pilot Program for Basic Research, National Natural Science Foundation of China, Grant/Award Number: 62205246; Science and Technology Commission of Shanghai Municipality, Grant/Award Number: 22ZR1432400

Abstract

Pixelated color convertor plays an immensely important role in next-generation display technologies. However, the inherent randomness of light propagation within the convertor presents a formidable challenge to reconcile the huge contradiction between excitation and outcoupling. Here, we demonstrate a bioinspired photonic waveguide pixelated color convertor (BPW-PCC) to realize directional excitation and outcoupling, which is inspired by an insect visual system. The lens array of BPW-PCC enables a focusing photonic waveguide that guides the excitation light and converges it on colloidal quantum dots; the directional channel provides a splitting photonic waveguide to enhance the outcoupling of photoluminescence light. Consequently, the excitation and outcoupling efficiency can be simultaneously improved at this judiciously designed pixelated color convertor with a thickness of 50 μm . By this strategy, ultrathin BPW-PCCs with 4.4-fold enhanced photoluminescence intensity have been demonstrated in micro-light-emitting diode devices and achieved a record-high luminous efficacy of 1600 $\text{lm W}^{-1} \text{mm}^{-1}$, opening a new avenue for efficient miniaturized displays.

KEYWORDS

bioinspired design, micro-light-emitting diodes, photonic waveguide, pixelated color convertors

Jiexin Li, Xinrui Ding and Yuzhi Shi contributed equally to this work.

This is an open access article under the terms of the [Creative Commons Attribution](https://creativecommons.org/licenses/by/4.0/) License, which permits use, distribution and reproduction in any medium, provided the original work is properly cited.

© 2024 The Author(s). FlexMat published by John Wiley & Sons Australia, Ltd on behalf of Nanjing University of Posts & Telecommunications.

1 | INTRODUCTION

Color converters, which can convert the color of photons through sequential absorption and emission, have been extensively studied and reached a plateau during the past decade.^{1,2} In particular, the emergence of miniaturized optoelectronics has enabled and boosted important application sectors, such as full-color micro-light-emitting diodes (micro-LED) displays, and thus reinforced the demand for pixelated color converters.^{3–8} So far, color converters have been developed primarily by excavating new materials with higher internal quantum efficiency and culminated in the synthesis and adoption of colloidal quantum dot (CQD),^{9–15} which was recently awarded the 2023 Nobel Prize in Chemistry. Currently, the patterning process of CQD-based micro-LEDs has reached a mature stage, but the device efficiency remains low. Various strategies have been given to improve the optical performance of color converters from excitation or outcoupling aspects. Examples include incorporating scatterers, such as random pore structures, nanorods, or metal-oxide nanoparticles, to enhance excitation efficiency (in absorbing the excitation photons and converting them to emissive photons), and adding Bragg reflectors,^{16–18} photonic crystals,^{19–21} localized surface plasmon resonance,^{22–24} photon management structures^{25,26} to increase outcoupling efficiency (in extracting the emitted photons from color converters). Particularly, we previously demonstrated that CQD/SBA-15 color converters significantly improve the outcoupling efficiency and achieve a record-high luminous efficacy of 206.8 lm W⁻¹ for CQD-based white LEDs.²⁵ However, conventional methods have manifested difficulties in addressing the inherent randomness of light propagation within color converters, thus failing to simultaneously improve excitation and outcoupling efficiency; such a challenge is more difficult to solve for thin-film pixelated color converters with an ultrahigh particle concentration.^{27–29} As illustrated in Figure 1A, the random propagation of the excitation light hinders the effective concentration on CQDs, limiting the production of emitted photons through radiative recombination and consequently restricting excitation efficiency. Similarly, the photoluminescence light emitted by the CQD also undergoes intrinsic propagation randomness. This situation results in its absorption by other surrounding CQDs, triggering non-radiative recombination, thus causing significant energy loss and a considerable reduction in outcoupling efficiency. As the external quantum efficiency (EQE)³⁰ of color converters is expressed as $EQE = \eta_{ex} \times \eta_{oc}$, where η_{ex} and η_{oc} are the excitation and outcoupling efficiency, respectively, the comprehensive realization of directional excitation and outcoupling is

crucial for simultaneously enhancing both excitation and outcoupling efficiency to achieve an improvement in the overall efficiency of color converters.

In this article, we propose a bioinspired photonic waveguide pixelated color convertor (BPW-PCC) to solve the contradiction between excitation and outcoupling, which is realized by a bioinspired optical structure from an insect visual system. Directional excitation and outcoupling can be realized in bioinspired photonic waveguide pixelated color converters (BPW-PCCs) to simultaneously improve excitation and outcoupling efficiency, boosting their overall efficiency. To demonstrate this concept, mesoporous silica Santa Barbara Amorphous-15 (SBA-15) nanoparticles and porous anodic alumina (PAA) membranes are employed as waveguide templates, and CdSe-based CQDs are selected as color converted materials to construct ultrathin BPW-PCCs (50 μm) through a universal template assemble approach. Finite difference time domain (FDTD) simulations are also utilized to gain a more comprehensive understanding of photonic waveguides in BPW-PCCs. Finally, we demonstrate that ultrathin BPW-PCCs with 4.4-fold enhanced photoluminescence intensity have been realized with micro-LED devices, achieving a record-high luminous efficacy of 1600 lm W⁻¹ mm⁻¹.

2 | RESULTS AND DISCUSSION

2.1 | Design of BPW-PCCs

In nature, compound eye insects, such as bees and dragonflies, demonstrate extraordinary visual imaging capabilities, including high visual resolution and sensitivity. Their unique visual system (Figure 1B left) exhibits formidable photon management: focusing light via the cornea and crystalline cone, and splitting light through the pigment cell channels, thus improving light reception and conversion efficiency. Inspired by the insect visual system, we designed a highly efficient ultrathin BPW-PCC with bioinspired optical structures (Figure 1B right), and supplemented the comparison between compound eye structure in insects³¹ and our color converter in Figure S1. The lens structure enables a focusing photonic waveguide that guides the excitation light to converge on CQDs, which enables the color conversion of excitation photons to largely increase excitation efficiency. Concurrently, the directional channel provides a splitting photonic waveguide to enhance the outcoupling of photoluminescence light, significantly increasing outcoupling efficiency. Directional excitation and outcoupling can be realized by our bioinspired photonic waveguide to boost the optical performance of color

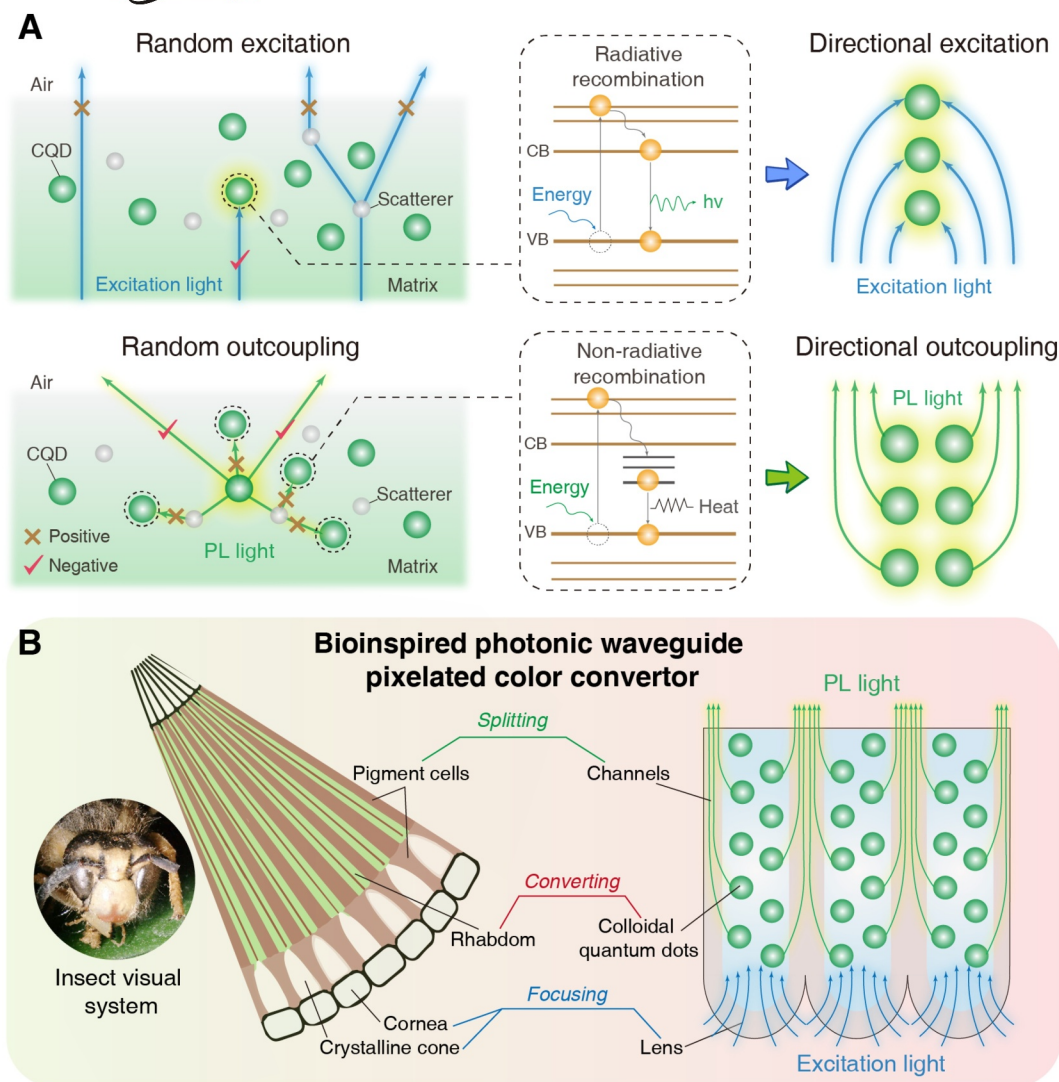


FIGURE 1 Design for bioinspired photonic waveguides. (A) Optical mechanism in thick-film Con-CCs with scatterers. Top left: excitation light (blue) entering Con-CCs is difficult to produce efficient excitation for CQDs due to the inherent randomness of light propagation, limiting the excitation efficiency. The top inset illustrates the transition process in CQDs upon the excitation and emission processes with radiative recombination. Top right: schematics of directional excitation to solve the random excitation issues. Bottom left: PL light (green) is hard to extract from color convertor, reducing the outcoupling efficiency. The bottom inset illustrates the transition process of non-radiative recombination, leading to a lot of energy loss. Bottom right: schematics of directional outcoupling to solve the random outcoupling issues. (B) BPW-PCCs. Insect visual system: focusing -cornea, crystalline cone; converting -rhabdom; splitting -pigment cells. BPW-PCCs: focusing -lens array; converting -CQDs; splitting -ordered channels. The bioinspired photonic waveguide allows for the directional excitation of CQDs to largely improve the excitation efficiency; concurrently, boost the outcoupling efficiency by mitigating energy loss absorbed by other CQDs. BPW-PCCs, bioinspired photonic waveguide pixelated color converters; Con-CCs, conventional color convertor; CQDs, colloidal quantum dots; PL, photoluminescence.

convertors. We conduct theoretical calculations to investigate the influence of the photonic waveguide on the photoluminescence intensity of BPW-PCCs (see Note S1 and Figure S2). The results reveal a trend wherein the photoluminescence intensity is significantly improved in response to an increase in excitation and outcoupling efficiency, corroborating our initial predictions. The photonic waveguides are crucial for achieving directional excitation and outcoupling in color

convertors, resulting in a significant enhancement of photoluminescence intensity and an improvement in luminous efficiency.

To demonstrate this concept, SBA-15 nanoparticles and PAA membranes are employed as waveguide templates, and CdSe-based CQDs are selected as color converted materials to construct BPW-PCCs. We proposed a universal template assembly approach to fabricate BPW-PCCs, as illustrated in Figure 2A (see detailed procedures

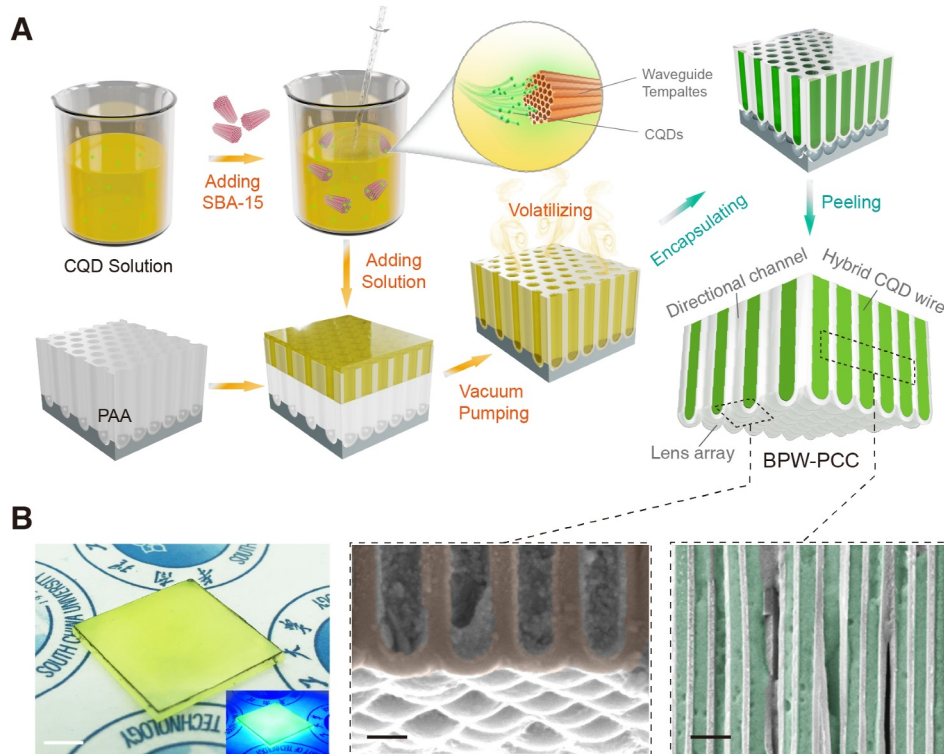


FIGURE 2 Fabrication and morphology of BPW-PCCs. (A) Diagram outlining the universal template assembly approach to fabricating BPW-PCCs and the corresponding structure schematic. (B) Optical photographs and cross-sectional SEM images of BPW-PCCs at the bottom and middle parts. The scale bars are 5 mm, 300 nm and 1 μm , respectively. BPW-PCCs, bioinspired photonic waveguide pixelated color converters; SEM, scanning electron microscope.

in the Experimental Section). Photographs of prepared BPW-PCCs exhibit a non-aggregated, homogeneous structure (Figure 2B left); in contrast, typical color converters with equivalent CQD material amounts display apparent aggregation (Figure S3). To further investigate the morphology of BPW-PCCs, transmission electron microscope (TEM) and scanning electron microscope (SEM) characterizations are conducted. The BPW-PCCs are composed of lens arrays, hybrid CQD wires and directional channels and their structural schematic and morphology are depicted in Figure 2A. The substrate-peeling process produces lens array (Figure 2B middle) at the bottom of BPW-PCCs, conferring a strong focusing photonic waveguide. The cross-sectional SEM images of blank PAA reveal empty pores organized in a near-hexagonal pattern (Figure S4). In contrast, lateral SEM images of BPW-PCCs demonstrate the presence of oriented hybrid CQD wires within the PAA structure. There are directional channels spaced between each hybrid CQD wire, providing an effective splitting photonic waveguide. The corresponding elemental mapping of BPW-PCCs is given in Figure S7. Al is distributed within the PAA framework, while Si, Cd, and Se from CQD/SBA-15 particles are located within PAA channels and exhibit homogeneous distributions.

2.2 | Optical analysis in BPW-PCCs

FDTD simulations are utilized to obtain a more comprehensive understanding of BPW-PCCs (Figure S8). The optical analysis is divided into two parts: one part is the focusing photonic waveguide caused by lens array to realize directional excitation of incident UV-blue light, and the other part is the splitting photonic waveguide based on directional channels to achieve directional outcoupling of green-red photoluminescence light. The unit BPW-PCC structure is illustrated in Figure 3A, and more details of simulations can be found in Note S2. The lens array at the bottom of BPW-PCCs as photon collectors efficiently help to focus excitation photons from air into hybrid CQD wires, largely enhancing the absorbance to increase excitation efficiency. To visualize a focusing photonic waveguide, dynamic processes of excitation light propagation in lens, planar and film structures are simulated, respectively. Note that the film structure corresponds to the conventional thin-film color converter, while the lens structure represents the BPW-PCC with focusing photonic waveguides; in contrast, the planar structure represents the BPW-PCC without focusing photonic waveguides. Animation of light propagation is available in Video S1, and electric field changes over time

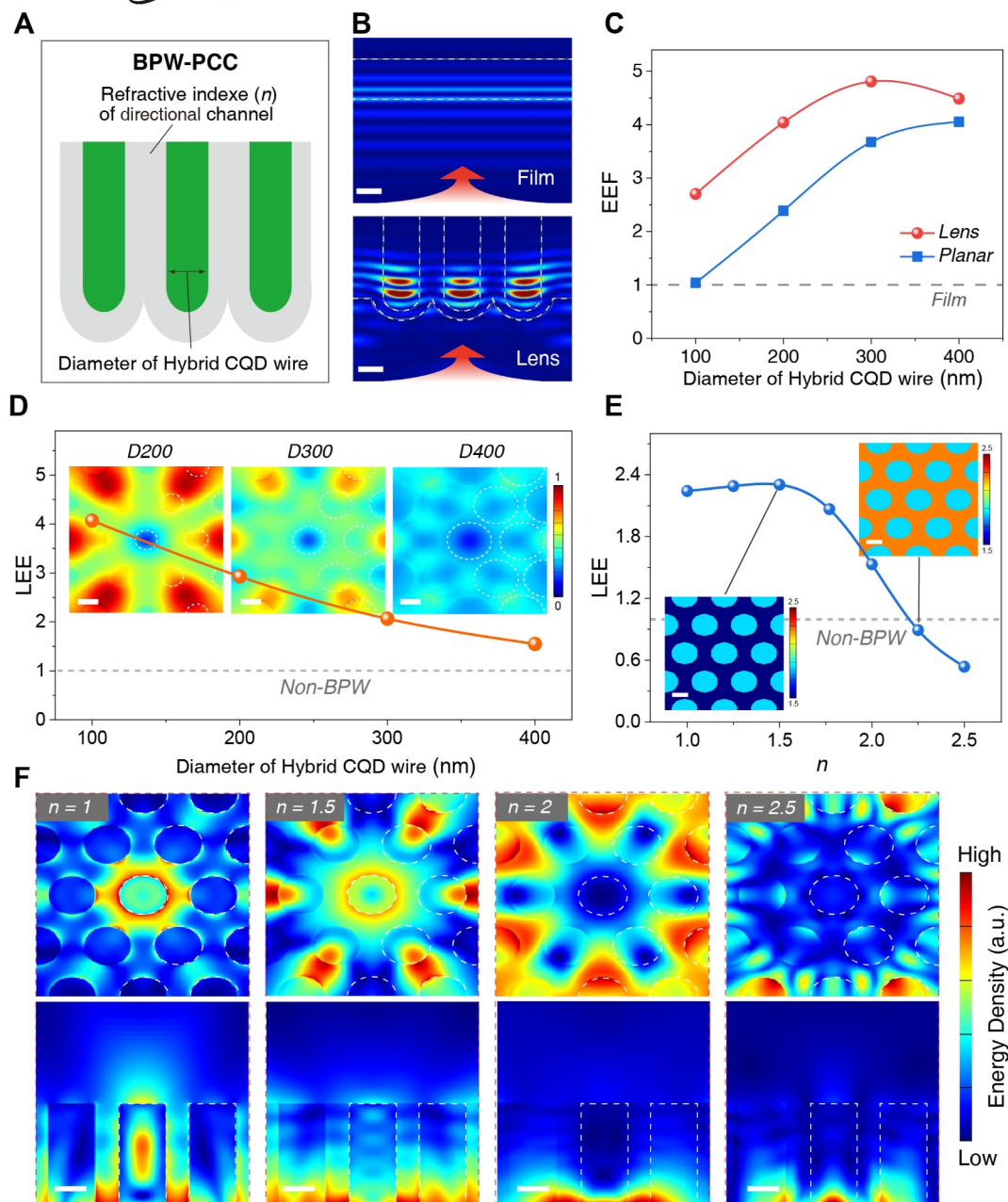


FIGURE 3 Optical analysis in BPW-PCCs. (A) Schematic of unit BPW-PCC structure. (B and C) Excitation analysis of a focusing photonic waveguide. (B) Energy density distributions of film and lens structure. (C) EEF of film structure and planar, lens structures with different diameters of hybrid CQD wire. (D–F) Outcoupling analysis of splitting photonic waveguide. (D) LEE of BPW-PCCs and energy density distributions with different diameters of hybrid CQD wire. (E) LEE of BPW-PCCs with different refractive indices of directional channels and (F) corresponding energy density distributions. The insets in (D) are the typical refractive index distributions. The scale bars are 200 nm. BPW-PCCs, bioinspired photonic waveguide pixelated color converters; CQD, colloidal quantum dot; EEF, excitation enhancement factor; LEE, light-extraction efficiency.

for different structures are summarized in Figure S9. Excitation light propagates upward and is focused into hybrid CQD wires a few femtoseconds after entering lens structures, exhibiting almost no change for the film case. Particularly, excitation light energy concentrates within the hybrid CQD wires as shown in Figure 3B. This focusing photonic waveguide can realize directional

excitation and has a dramatic impact on the excitation efficiency of BPW-PCCs. The excitation enhancement factor (EEF), defined as the ratio of absorbance for different structures to that for film structure, is used to determine the excitation enhancement. Figure 3C shows the EEF of film structure and planar, lens structure with different diameters of hybrid CQD wire. The EEF for

planar structures with different diameters exceeds that for film structures, indicating that the color convertors with hybrid CQD wire contribute to enhanced excitation. The decreasing discrepancy between the lens and planar structures with increasing diameter indicates that the decreasing enhancement effect is due to the hybrid CQD wires almost filling the entire BPW-PC at sufficiently large diameters. Compared to the film structure in conventional color convertors (Con-CCs), lens structure in BPW-PCC exhibits several-fold EEF, which demonstrates that the focusing photonic waveguide further helps to largely enhance the excitation efficiency.

The outcoupling of BPW-PCCs is analyzed using a numerical method based on plane wave expansion with interface reflection and angular distribution to determine the light power outcoupled into the air.³² A reference structure without bioinspired photonic waveguides (non-BPW) is also established for comparison. We use light-extraction efficiency (LEE), defined as the transmittance ratio of photoluminescence light in BPW-PCC to that in non-BPW structure. As shown in Figure 3D, the LEE value exceeds 1, indicating more photoluminescence light can be extracted from color convertors compared to non-BPW structure. This is attributed to the splitting photonic waveguide originated from the directional channel, allowing emitted photons to bypass hybrid CQD wire to reduce the non-radiative recombination loss. A pathway for photon extraction is generated to facilitate higher outcoupling efficiency. The LEE decreases with increasing diameter of hybrid CQD wire, which indicates an increased energy consumption within the structures, thereby reducing the outcoupling of photoluminescence light. In particular, the increase in diameter of hybrid CQD wires results in a compression of inter-wire spaces, reducing the proportion of directional channels and simultaneously increasing the non-radiative recombination loss in hybrid CQD wires, which consequently affects the outcoupling of photoluminescence. The inset energy density distributions confirm that photoluminescence light is primarily confined to directional channels in BPW-PCC, while the energy in directional channel significantly decreases with increasing diameter. The photoluminescence intensity is simultaneously affected by the excitation and outcoupling efficiency of color convertors; thus, the optimal diameter of hybrid CQD wire ($D = 300$ nm) is ultimately selected for succeeding simulations and experiments. We also systematically investigate the refractive index (n) of the directional channel to elucidate the origin of the splitting photonic waveguide in BPW-PCC. As shown in Figure 3E, LEE increases with n and reaches a maximum value of 2.4 at $n = 1.5$, indicating significantly enhanced outcoupling of photoluminescence light. For $n > 1.5$, however, LEE

sharply decreases below that of the non-BPW structure. Energy density distributions (Figure 3F) provide an insight into this trend. At $n = 1$, the energy has already been split into directional channel, yet a portion remains in hybrid CQD wires, reflecting limited outcoupling of emitted photons. Nevertheless, the short optical path-length enabled relatively efficient light extraction. In contrast, $n \approx 1.5$ enables more emitted photons to propagate into the channel and ultimately escape BPW-PCC, further enhancing LEE. However, further increasing n dramatically enhances lateral propagation and absorption by hybrid CQD wires, thereby resulting in severe energy loss and a reduction in LEE. Overall, a matched refractive index of directional channel is required to generate an effective splitting photonic waveguide for enhancing the extraction of emitted photons, thereby achieving a significant boost in outcoupling efficiency.

2.3 | Optical performance and micro-LED display application

To integrate with miniaturized optoelectronic devices, color convertors must be precisely patterned with a high resolution while maintaining an ultralow thickness.^{27,33–36} Despite significant progress in miniaturization integration, the luminous efficacy (the ratio of luminous flux to electrical power) of devices using ultrathin color convertors remains disappointingly low and hard to measure, which is far lower than traditional macro lighting devices (>200 lm W⁻¹).^{25,37} In general, the luminous efficacy of color convertors is related to their thickness, simultaneously achieving enhanced excitation and outcoupling efficiency becomes increasingly challenging as the thickness decreases owing to denser distributions of color converted materials, impeding their practical applications in micro-LED displays. However, our proposed BPW-PCCs can maintain ultrathin thickness while largely enhancing their luminous efficacy. As illustrated in Figure 4A, Con-CCs, only dispersing CQD in polymer matrix, always necessitate a substantial thickness (up to 1000 μ m) to facilitate adequate color conversion. Conversely, BPW-PCC exhibits a markedly reduced thickness (approximately 50 μ m), rendering it more amenable for integration with micro-LED devices. The bidirectional photoluminescence spectra of BPW-PCCs confirm that their strong photoluminescence intensity asymmetry is attributed to the directivity of the photonic waveguide originating from the unique bioinspired optical structures (detailed discussion can be found in Note S3 and Figure S10). We investigate the absorbance and photoluminescence intensity enhancement of BPW-PCCs compared to Con-CCs and NP-CCs (only dispersing

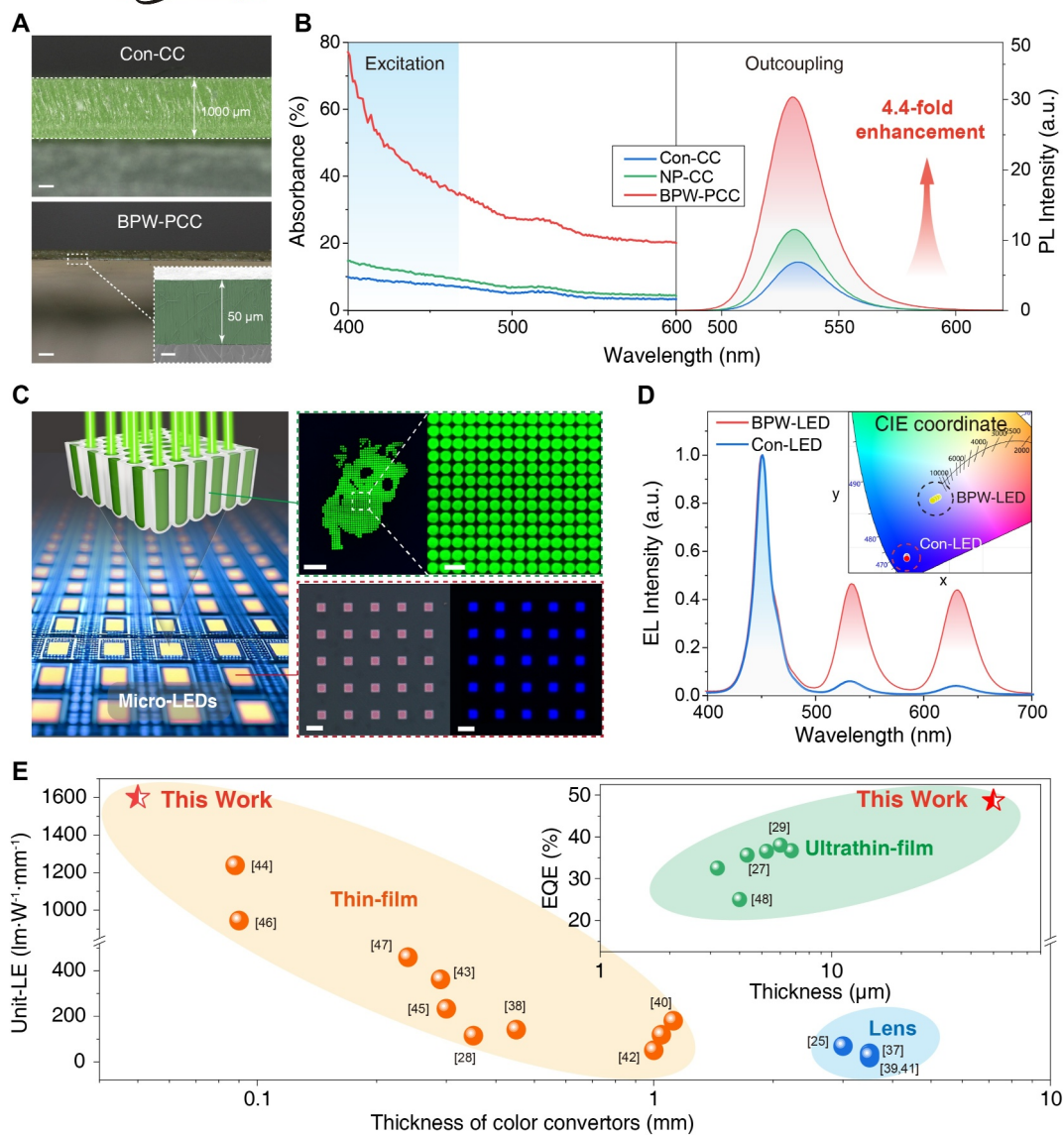


FIGURE 4 Optical performances and micro-LED display application. (A) Thickness comparison of conventional color converter (top) and BPW-PCC (bottom). (B) Photoluminescence and absorbance performances of BPW-PCCs. Absorbance (left) and photoluminescence spectrum (right) comparison of Con-CC, NP-CC and BPW-PCC. (C) Schematic of efficient micro-LED display application with BPW-PCCs. Fluorescent images of patterned BPW-PCCs (top) and micro-LED devices (bottom). The scale bar is 2 mm for the fluorescent images, 300 μm for the magnification, and the scale bar is 150 μm for the micro-LED devices. (D) EL spectra and CIE coordinates comparison of Con-LED and BPW-LED. (E) Unit-LE and EQE comparisons. BPW-PCCs, bioinspired photonic waveguide pixelated color converters; Con-CC, conventional color converter; Con-LED, conventional LED; EL, electroluminescence; EQE, external quantum efficiency; NP-CC, nanoparticle color converter; unit-LE, luminous efficacy per unit thickness.

CQD/SBA-15 nanoparticles in polymer matrix), all color converters have the same thickness and identical amount of CQDs. Their absorbance and photoluminescence spectra are measured as shown in Figure 4B. The absorbance of BPW-PCCs in the excitation spectrum range is significantly increased due to the implementation of directional excitation. These results well confirm the concept of a focusing photonic waveguide, as discussed in optical analysis, and contribute to a substantial enhancement in excitation efficiency. The excitation light is

focused by the lens array on hybrid CQD wires to enhance the absorbance of ultrathin color converters, reaching a performance level comparable to thick-film color converters in millimeters. Furthermore, BPW-PCCs yield the highest photoluminescence intensity despite having the same amount of CQDs and thickness as other color converters. The introduction of CQD/SBA-15 particles in NP-CC enhances photoluminescence intensity compared to Con-CCs (1.67-fold), consistent with our previous studies.²⁵ In contrast, the bioinspired photonic

waveguides endow BPW-PCCs with an enhanced photoluminescence intensity of up to 4.4-fold. This significant enhancement in photoluminescence intensity is mainly attributed to the simultaneously enhanced excitation and outcoupling of BPW-PCCs, boosting their overall efficiency.

To further verify the feasibility of BPW-PCCs in micro-LED displays, large-area patterned displays of different colors and pixel sizes are shown in Figure 4C and Figure S11, exhibiting excellent uniformity and luminescence. We also investigate the optical performances of devices under different injection currents, with electroluminescence (EL) spectra at a typical injection current shown in Figure 4D. The integrated intensity of green and red light emitted from BPW-LEDs is greatly enhanced compared to Con-LEDs under the same conditions. Color coordinates of BPW-LEDs are concentrated in the near-white light region despite a thickness of only 50 μm , while Con-LEDs remain in the blue light region. The color proportions are also provided in Figure S13 and Note S4 to confirm the efficient color conversion of BPW-PCCs. Furthermore, luminous fluxes and corresponding luminous efficacies, obtained by dividing luminous flux by electrical power, for BPW-LEDs and Con-LEDs are presented in Figure S14. The results demonstrate that the incorporation of bioinspired photonic waveguides can facilitate an enhancement in luminous efficacy by an approximate factor of 45% owing to the stronger excitation and outcoupling of BPW-PCCs. To compare the stability and lifespan of BPW-LEDs and Con-LEDs, we have performed harsh aging tests for these devices without bonding on the heat sink and only with ambient convention; the injection current was 100 mA. Luminous flux maintenance (LFM) results for these devices are shown in Figure S15, which refers to the ratio of aging time-dependent luminous flux to initial luminous flux. Evidently, the LFM of BPW-LED remained almost constant in the initial stage, with only a slight decrease in the later period; in contrast, Con-LED rapidly declined before eventually stabilizing. These results indicate that BPW-LED exhibits superior stability and a longer lifespan compared to conventional devices.

As discussed above, a decrease in thickness results in a corresponding decrease in luminous efficacy, complicating direct comparisons of luminous efficacy between color convertors of varying thicknesses. To facilitate such comparisons, luminous efficacy per unit thickness (unit-LE) is proposed and defined as the ratio of device luminous efficacy to the thickness of color convertors. A larger unit-LE indicates a more highly efficient and ultrathin color convertor. For convenience, the maximum unit-LE of BPW-LED is marked in Figure 4E for comparison with various color convertors in previous studies.

In general, LED devices can be divided into several main categories according to the thickness of color convertors: lens, thin-film, and ultrathin-film types. Color convertors can be formed into lens shapes to maximize device efficiency, but unit-LE of lens type devices is extremely low due to their large thickness, which is generally adopted in macro devices. Thin-film type devices have advantages in thickness control, ranging from tens of microns to a few millimeters, but most unit-LEs for thin-film type devices are $<400 \text{ lm W}^{-1} \text{ mm}^{-1}$, indicating difficulty in meeting demand for efficient color conversion. Our work achieves unit-LE of $1600 \text{ lm W}^{-1} \text{ mm}^{-1}$ which is a record efficacy in reported studies,^{25,28,37–47} which we summarize in Table S1. Ultrathin-film type devices have a thickness of color convertors ranging from a few microns to tens of microns, they have ultrahigh concentration CQD deposition with severe intrinsic absorption limitations. The luminance of ultrathin-film type devices is too low to be measured and difficult for practical applications. Thus, their overall efficiency is usually characterized by EQE. To compare with ultrathin film-type devices fairly, the quantum efficiencies of BPW-LEDs are measured, and corresponding EQE values are calculated according to previous studies.²⁷ More details can be found in Note S5. As shown in the inset of Figure 4E, ultrathin-film type devices in previous reports have a low EQE of 25%–40%.^{27,29,48} In contrast, our work achieves high luminance (equivalent to commercial LED devices) and an EQE of 48.6%, consistently higher than ultrathin film-type devices. These results demonstrate that the photonic waveguides designed by bioinspired optical structures endow high excitation and outcoupling of color convertors, leading to a largely enhanced luminous efficacy of miniaturized devices.

3 | CONCLUSION

We have demonstrated a photonic waveguide concept to solve the inherent randomness of light propagation in color convertors. The highly efficient BPW-PCCs designed by bioinspired optical structures realize directional excitation and outcoupling to simultaneously improve excitation and outcoupling efficiency, boosting the overall efficiency of color convertors. To demonstrate this concept, SBA-15 nanoparticles and PAA membranes are employed as waveguide templates, and CdSe-based CQDs are selected as color converted materials to construct BPW-PCCs through a universal template assemble approach. Optical analyses reveal that the lens array enables a focusing photonic waveguide that guides the excitation light to converge on CQDs; concurrently, the directional channel provides a splitting photonic

waveguide to enhance the outcoupling of photoluminescence light. By using this strategy, we demonstrate that BPW-PCCs with 4.4-fold enhanced photoluminescence intensity have been realized with micro-LED devices to achieve a record-high luminous efficacy per unit thickness of $1600 \text{ lm W}^{-1} \text{ mm}^{-1}$. In addition, the color converter thickness of $50 \mu\text{m}$ still limits its applications in smaller-scale miniaturized devices. The overall thickness of our BPW-PCC is primarily determined by the PAA membrane thickness; thus, the thickness can be further reduced by optimizing the fabrication process of PAA membranes, thereby making it suitable for miniaturized devices. We believe our bio-inspired photonic waveguides can be applied for photon managements in perovskite, MoS_2 , and InP based CQDs and facilitate designing nano/micro-photonic crystal structures to further improve efficiency. Our approach also provides a universal way to realize high-performance color converters for future applications in miniature spectrometers, wide-color-gamut augmented reality/virtual reality displays and wearable flexible photoelectric sensors.

4 | EXPERIMENTAL SECTION

4.1 | Materials

Green and red CdSe-based CQDs were purchased from Beijing Beida Jubang Science & Technology Co., Ltd. Their peak emission wavelengths are 530 and 625 nm, respectively, and both have a photoluminescence quantum yield of $\sim 85\%$. Polydimethylsiloxane (PDMS) was purchased from Dow Corning. Chlorobenzene as the assisted solvent during CQD dispersion was purchased from Aladdin Reagents. SBA-15 particles were purchased from Nanjing XFNANO Co., Ltd.; their mean pore size was 11 nm. PAA membranes (mean pore size, 400 nm; mean pore depth, $50 \mu\text{m}$) were purchased from Shanghai Shangmu Technology Co. Ltd. Blue micro-LED devices (pixel size: $80 \mu\text{m} \times 80 \mu\text{m}$, pixel pitch: $160 \mu\text{m}$) were purchased from Foshan NationStar Optoelectronics Co., Ltd.; the peak emission wavelength was 455 nm.

4.2 | CQD/SBA-15 particles preparation

The Wet-mixing and sonication methods were used for nanoscale assemble between CQDs and SBA-15 particles, leading to CQD/SBA-15 particles. The CdSe-based CQDs were mixed with SBA-15 particles at a specific mass ratio

in a chlorobenzene solution; the CQD concentration in the solution was kept at 5 mg mL^{-1} . Then, the mixture was mixed uniformly with ultrasound for seconds and moved to a planetary mixer, until the chlorobenzene was entirely volatilized.

4.3 | BPW-PCCs fabrication

A repeated vacuum-deposition process was employed for inducing the assembly between CQD/SBA-15 particles and PAA membrane. The BPW-PCCs were fabricated using the following steps: (1) CQD/SBA-15 particles were dispersed in a chlorobenzene solution, and then deposited onto an PAA chip; (2) the PAA chip was transferred to a vacuum desiccator, and pimpled for 3 h, to remove air from the pores and guide the solution into PAA channels while inducing the deposition of CQD/SBA-15 particles and volatilizing the solvent, for obtaining hybrid CQD wires; (3) the PAA chip was wiped with tissue, to completely remove the top residue of particles; (4) the above steps were performed repeatedly; (5) the encapsulation process involves protecting the hybrid CQD wire using UV-curable adhesive to prevent damage during the subsequent peeling procedure; (6) chemical wet etching was constructed to eliminate aluminum substrates in PAA chips, obtaining the BPW-PCCs. Note that the substrate-peeling process produced lens array at the bottom of BPW-PCCs.

4.4 | Patterned BPW-PCCs

The patterned color converter is realized through inkjet printing method during the fabrication process. Localized deposition of the CQD solution onto PAA substrate enables the patterning of BPW-PCCs. The resolution of this patterning is determined by the parameters of inkjet printing process and the pore dimensions of PAA.

4.5 | Integration with micro-LEDs

For individual micro-LED devices, the color converter is segmented into pixelated units and assembled onto each device. For micro-LED arrays, a patterned color converter is directly integrated with Micro-LED array module, with the pattern configured to correspond to the distribution of Micro-LED array. Note that the inkjet printing method are used to fabricate patterned BPW-PCCs, allowing to produce color converters precisely tailored to the micro-LEDs with various dimensions.

4.6 | Measurement and characterization

The morphologies of the CQDs, SBA-15 nanoparticles and CQD/SBA-15 particles were measured using a TEM instrument (Bruker). The morphologies of the prepared BPW-PCCs and PAA membranes were characterized using scanning electron microscopy (SEM, Zeiss, Merlin). The absorbance and photoluminescence spectra of the BPW-PCCs were measured using an ultraviolet-visible (UV-vis) spectrometer (Shimadzu). The optical performances of white LEDs were measured by an integrating sphere system from Instrument Systems, and the injection current was provided by a power source from Keithley.

ACKNOWLEDGMENTS

This research is supported by National Key R & D Program of China (2021YFB3600205); National Natural Science Foundation of China (52105443); Guangdong Provincial Key R&D Program (2022B0101090002) and Natural Science Foundation of Guangdong Province (2022A1515011059). Yuzhi Shi acknowledges the National Key Research and Development Program of China (No. 2023YFF0613600), the Shanghai Pilot Program for Basic Research, National Natural Science Foundation of China (No. 62205246), and Science and Technology Commission of Shanghai Municipality (No. 22ZR1432400).

AUTHOR CONTRIBUTIONS

Jiexin Li: Data curation; formal analysis; investigation; methodology; visualization; writing—original draft; writing—review & editing. **Xinrui Ding:** Data curation; formal analysis; investigation; methodology; visualization; writing—original draft; writing—review & editing. **Yuzhi Shi:** Data curation; formal analysis; investigation; methodology; visualization; writing—original draft; writing—review & editing. **Jiasheng Li:** Conceptualization; funding acquisition; investigation; methodology; project administration; visualization; writing—original draft; writing—review & editing. **Zihao Deng:** Investigation; Methodology; writing—review & editing. **Jiayong Qiu:** Investigation; methodology; writing—review & editing. **Jinhui Zhang:** Investigation; methodology; writing—review & editing. **Wei Luo:** Investigation; methodology; writing—review & editing. **Guanwei Liang:** Investigation; methodology; writing—review & editing. **Long Zhao:** Investigation; methodology; writing—review & editing. **Yong Tang:** Formal analysis; investigation; writing—review & editing. **Ai Qun Liu:** Conceptualization; formal analysis; project administration; supervision; visualization; writing—original draft;

writing—review & editing. **Zongtao Li:** Conceptualization; funding acquisition; project administration; resources; supervision; writing—original draft; writing—review & editing.

CONFLICT OF INTEREST STATEMENT

The authors declare no conflict of interests.

DATA AVAILABILITY STATEMENT

The data that support the findings of this study are available from the corresponding author upon reasonable request.

ORCID

Yuzhi Shi  <https://orcid.org/0000-0002-9041-0462>

REFERENCES

1. E. F. Schubert, J. K. Kim, *Science* **2005**, *308*, 1274.
2. C. Feldmann, T. Jüstel, C. R. Ronda, P. J. Schmidt, *Adv. Funct. Mater.* **2003**, *13*, 511.
3. L. Yi, B. Hou, H. Zhao, X. Liu, *Nature* **2023**, *618*, 281.
4. W. Chang, J. Kim, M. Kim, M. W. Lee, C. H. Lim, G. Kim, S. Hwang, J. Chang, Y. H. Min, K. Jeon, Y. H. Choi, J. S. Lee, *Nature* **2023**, *617*, 287.
5. J. Yang, D. Hahm, K. Kim, S. Rhee, M. Lee, S. Kim, J. H. Chang, H. W. Park, J. Lim, M. Lee, J. Bang, H. Ahn, J. H. Cho, J. Kwak, B. Kim, C. Lee, W. K. Bae, M. S. Kang, *Nat. Commun.* **2020**, *11*, 2874.
6. Y. Wang, I. Fedin, H. Zhang, D. V. Talapin, *Science* **2017**, *357*, 385.
7. J.-S. Park, J. Kyhm, H. H. Kim, S. Jeong, J. Kang, S.-e. Lee, K.-T. Lee, K. Park, N. Barange, J. Han, J. D. Song, W. K. Choi, I. K. Han, *Nano Lett.* **2016**, *16*, 6946.
8. V. Wood, M. J. Panzer, J. Chen, M. S. Bradley, J. E. Halpert, M. G. Bawendi, V. Bulović, *Adv. Mater.* **2009**, *21*, 2151.
9. V. L. Colvin, M. C. Schlamp, A. P. Alivisatos, *Nature* **1994**, *370*, 354.
10. A. P. Alivisatos, *Science* **1996**, *271*, 933.
11. Q. Sun, Y. A. Wang, L. S. Li, D. Wang, T. Zhu, J. Xu, C. Yang, Y. Li, *Nat. Photonics* **2007**, *1*, 717.
12. C. Dang, J. Lee, C. Breen, J. S. Steckel, S. Coe-Sullivan, A. Nurmikko, *Nat. Nanotechnol.* **2012**, *7*, 335.
13. Y. Yang, Y. Zheng, W. Cao, A. Titov, J. Hyvonen, J. R. Manders, J. Xue, P. H. Holloway, L. Qian, *Nat. Photonics* **2015**, *9*, 259.
14. X. Dai, Y. Deng, X. Peng, Y. Jin, *Adv. Mater.* **2017**, *29*, 1607022.
15. N. Ahn, C. Livache, V. Pinchetti, H. Jung, H. Jin, D. Hahm, Y.-S. Park, V. I. Klimov, *Nature* **2023**, *617*, 79.
16. S.-W. H. Chen, C.-C. Shen, T. Wu, Z.-Y. Liao, L.-F. Chen, J.-R. Zhou, C.-F. Lee, C.-H. Lin, C.-C. Lin, C.-W. Sher, *Photonics Res.* **2019**, *7*, 416.
17. H.-V. Han, H.-Y. Lin, C.-C. Lin, W.-C. Chong, J.-R. Li, K.-J. Chen, P. Yu, T.-M. Chen, H.-M. Chen, K.-M. Lau, H. C. Kuo, *Opt. Express* **2015**, *23*, 32504.
18. H.-Y. Lin, C.-W. Sher, D.-H. Hsieh, X.-Y. Chen, H.-M. P. Chen, T.-M. Chen, K.-M. Lau, C.-H. Chen, C.-C. Lin, H.-C. Kuo, *Photonics Res.* **2017**, *5*, 411.

19. T. Baba, *Nat. Photonics* **2008**, *2*, 465.
20. J. Lee, K. Min, Y. Park, K. S. Cho, H. Jeon, *Adv. Mater.* **2018**, *30*, 1703506.
21. K. Min, S. Choi, Y. Choi, H. Jeon, *Nanoscale* **2014**, *6*, 14531.
22. D. Nepal, L. F. Drummy, S. Biswas, K. Park, R. A. Vaia, *ACS Nano* **2013**, *7*, 9064.
23. P. Pompa, L. Martiradonna, A. D. Torre, F. D. Sala, L. Manna, M. De Vittorio, F. Calabi, R. Cingolani, R. Rinaldi, *Nat. Nanotechnol.* **2006**, *1*, 126.
24. L. Zhang, Y. Song, T. Fujita, Y. Zhang, M. Chen, T. H. Wang, *Adv. Mater.* **2014**, *26*, 1289.
25. J.-S. Li, Y. Tang, Z.-T. Li, J.-X. Li, X.-R. Ding, B.-H. Yu, S.-D. Yu, J.-Z. Ou, H.-C. Kuo, *ACS Nano* **2020**, *15*, 550.
26. J. Li, Y. Tang, Z. Li, X. Ding, B. Yu, L. Lin, *ACS Appl. Mater. Interfaces* **2019**, *11*, 18808.
27. J. Bae, Y. Shin, H. Yoo, Y. Choi, J. Lim, D. Jeon, I. Kim, M. Han, S. Lee, *Nat. Commun.* **2022**, *13*, 1862.
28. Z. Bao, J.-W. Luo, Y.-S. Wang, T.-C. Hu, S.-Y. Tsai, Y.-T. Tsai, H.-C. Wang, F.-H. Chen, Y.-C. Lee, T.-L. Tsai, R. J. Chung, R. S. Liu, *Chem. Eng. J.* **2021**, *426*, 130849.
29. S.-W. H. Chen, Y.-M. Huang, K. J. Singh, Y.-C. Hsu, F.-J. Liou, J. Song, J. Choi, P.-T. Lee, C.-C. Lin, Z. Chen, J. Han, T. Wu, H. C. Kuo, *Photonics Res.* **2020**, *8*, 630.
30. T.-Y. Lee, Y. Park, H. Jeon, *Nat. Commun.* **2023**, *14*, 6661.
31. Q.-X. Chen, B.-Z. J. P. O. Hua, *PLoS One* **2016**, *11*, e0156970.
32. S.-S. Meng, Y.-Q. Li, J.-X. Tang, *Org. Electron.* **2018**, *61*, 351.
33. D. A. Miller, *Science* **2023**, *379*, 41.
34. M. K. Choi, J. Yang, K. Kang, D. C. Kim, C. Choi, C. Park, S. J. Kim, S. I. Chae, T.-H. Kim, J. H. Kim, T. Hyeon, *Nat. Commun.* **2015**, *6*, 7149.
35. T.-H. Kim, D.-Y. Chung, J. Ku, I. Song, S. Sul, D.-H. Kim, K.-S. Cho, B. L. Choi, J. Min Kim, S. Hwang, *Nat. Commun.* **2013**, *4*, 2637.
36. T.-H. Kim, K.-S. Cho, E. K. Lee, S. J. Lee, J. Chae, J. W. Kim, D. H. Kim, J.-Y. Kwon, G. Amaratunga, S. Y. Lee, B. L. Choi, Y. Kuk, K. Kim, *Nat. Photonics* **2011**, *5*, 176.
37. A. Onal, G. O. Eren, S. Sadeghi, R. Melikov, M. Han, O. Karatum, M. S. Ozer, H. Bahmani Jalali, I. B. Dogru-Yuksel, I. Yilgor, Ö. Metin, S. Nizamoglu, *ACS Photonics* **2022**, *9*, 1304.
38. K. Han, J. Heo, W. J. Chung, *Opt. Mater.* **2021**, *111*, 110545.
39. S. Sadeghi, R. Melikov, H. B. Jalali, S. Nizamoglu, *IEEE Trans. Electron Devices* **2019**, *66*, 4784.
40. C. Y. Kang, C. H. Lin, C. H. Lin, T. Y. Li, S. W. Huang Chen, C. L. Tsai, C. W. Sher, T. Z. Wu, P. T. Lee, X. Xu, M. Zhang, C. Ho, J. He, H. Kuo, *Adv. Sci.* **2019**, *6*, 1902230.
41. S. Sadeghi, B. G. Kumar, R. Melikov, M. M. Aria, H. B. Jalali, S. Nizamoglu, *Optica* **2018**, *5*, 793.
42. X. Di, Z. Hu, J. Jiang, M. He, L. Zhou, W. Xiang, X. Liang, *Chem. Commun.* **2017**, *53*, 11068.
43. S. Abe, J. J. Joos, L. I. Martin, Z. Hens, P. F. Smet, *Light Sci. Appl.* **2017**, *6*, e16271.
44. Q. Zhou, Z. Bai, W. g. Lu, Y. Wang, B. Zou, H. Zhong, *Adv. Mater.* **2016**, *28*, 9163.
45. B. Xie, R. Hu, X. Yu, B. Shang, Y. Ma, X. Luo, *IEEE Photonics Technol. Lett* **2016**, *28*, 1115.
46. J.-Y. Lien, C.-J. Chen, R.-K. Chiang, S.-L. Wang, *Opt. Express* **2016**, *24*, A1021.
47. K. J. Chen, H. C. Chen, K. A. Tsai, C. C. Lin, H. H. Tsai, S. H. Chien, B. S. Cheng, Y. J. Hsu, M. H. Shih, C. H. Tsai, H. Kuo, *Adv. Funct. Mater.* **2012**, *22*, 5138.
48. E. Lee, R. Tangirala, A. Smith, A. Carpenter, C. Hotz, H. Kim, J. Yurek, T. Miki, S. Yoshihara, T. Kizaki, A. Ishizuka, I. Kiyoto, *SID Symp. Dig. Tech. Pap.* **2018**, *49*, 525.

SUPPORTING INFORMATION

Additional supporting information can be found online in the Supporting Information section at the end of this article.

How to cite this article: J. Li, X. Ding, Y. Shi, J. Li, Z. Deng, J. Qiu, J. Zhang, W. Luo, G. Liang, L. Zhao, Y. Tang, A. Q. Liu, Z. Li, *FlexMat* **2024**, *1*, 258. <https://doi.org/10.1002/flm2.33>